JPP Journal of Pharmacy and Pharmacology

JPP 2010, 62: 422–429

Received October 29, 2009
Accepted January 7, 2010
DOI 10.1211/jpp/62.04.0003
ISSN 0022-3573

Research Paper

Preparation and in-vitro/in-vivo evaluation of surface-modified poly (lactide-co-glycolide) fluorescent nanoparticles

Sarala Pamujula[a], Sidhartha Hazari[b], Gevoni Bolden[a], Richard A. Graves[a], Dakshina M. Devanga Chinta[a], Srikanta Dash[b], Vimal Kishore[a] and Tarun K. Mandal[a]

[a]Center for Nanomedicine and Drug Delivery, Xavier University College of Pharmacy, New Orleans, LA, USA and [b]Tulane University Health Sciences Center, New Orleans, LA, USA

Abstract

Objective The aim was to develop biodegradable nanoparticles suitable for cellular delivery of chemotherapeutic drugs.

Methods Poly (lactide-co-glycolide) (PLGA) nanoparticles were prepared using a modified solvent evaporation method. Chitosan and calcium chloride were tested as surface modifiers. Coumarin-6 was incorporated into some formulations as a fluorescent marker.

Key findings The median size of the particles was between 400 nm and 7 μm, and scanning electron microscope pictures showed that the particles were smooth and spherical. The zeta potentials of the particles with and without surface modifier ranged between −25.7 mV and −7.0 mV, respectively. Fluorescence microscopy and flow cytometry (FACS) analysis showed that smaller surface-modified particles were efficiently internalised by neoplastic 4T1 cells. Image analysis of frozen tissue sections from Balb/c mice given nanoparticles via the tail vein showed that the particles were distributed preferentially into the lungs, followed by the liver, spleen, kidney and heart.

Conclusions Chitosan-modified PLGA nanoparticles showed significant uptake by neoplastic 4T1 cells, and were distributed to several major organs frequently seen as sites of cancer metastasis in mice.

Keywords biodistribution; chitosan; coumarin-6; nanoparticles; PLGA

Introduction

In pharmacy and medicine, engineered nanoparticles are defined as submicroscopic particles between 1 and 100 nm in size, although some define them as up to 1 micron.[1] In cancer therapy, nanoparticle delivery systems provide efficient delivery of therapeutic and diagnostic substances with a reduced risk compared with conventional cancer therapies.[2,3] These formulations are constructed to take advantage of fundamental cancer morphology and modes of development, such as rapid proliferation of cells, antigen expression and leaky tumour vasculature.[4] The two most significant characteristics that influence the distribution of these particles within the body are particle size and surface charge.[5] Relatively small and surface-modified particles show longer circulation times, possibly taking advantage of leaky tumour vasculature, whereas positively charged particles show greater cell penetration through adsorptive endocytosis.[6,7]

Nanoparticles can be formulated from a variety of materials and have been engineered to carry an array of substances in a controlled and targeted manner.[8] Nanoparticles used in anticancer therapies may be composed, in whole or in part, of various lipids and natural and synthetic polymers. Synthetic polymers commonly used to prepare nanoparticles for drug delivery are biodegradable. The most extensively used is poly (lactide-co-glycolide) (PLGA), which has attracted most attention because the biodegradation rate of this copolymer is easily controlled by altering the proportions of lactide and glycolide.[9] These polymers have been used with numerous drugs for parenteral delivery and have been shown to be biocompatible. Once-a-month injectable particles of leuprolide acetate using PLGA have been described.[10]

Correspondence: MandalTarun K. Collegeof Pharmacy, Xavier University of Louisiana, 1 Drexel Dr., New Orleans, LA 70125-1098, USA. E-mail: tmandal@xula.edu

In efforts to improve cellular delivery, several investigators[5] have modified the zeta potential of these nanoparticles by adding cationic excipients during the preparation. Calcium chloride and chitosan are two surface modifiers commonly used to achieve cationic particles.[11,12] These cationic particles show improved cellular targeting and can also cross the blood–brain barrier.[13] Calcium chloride also acts as a stabiliser in PLGA formulations. Zhang and co-workers have recently used calcium chloride as a stabiliser during the preparation of peptide-loaded PLGA microspheres by solvent evaporation.[14] The presence of calcium chloride in both the primary emulsion and the outer aqueous phase improved the efficiency of encapsulation and inhibited acylation of octreotide.

Several investigators have studied the intracellular and tissue distribution of nanoparticles in order to elucidate the mechanism of enhanced therapeutic efficiency of drug-loaded nanoparticles.[15–18] Our long-term objective is to develop biodegradable nanoparticles suitable for cellular delivery of chemotherapeutic drugs. This report focuses on the preparation of surface-modified coumarin-6 encapsulated PLGA nanoparticles, and in-vitro/in-vivo evaluation using 4T1 cells, a murine metastatic breast cancer cell line, and Balb/c mice.

Materials and Methods

Materials

PLGA 50 : 50 (RG 506; inherent viscosity 0.8 dl/g; molecular weight 100 000 Da) was obtained from Boehringer Ingelheim, Germany). The surfactant L-α phosphatidylcholine was from Avanti Polar Lipids, Inc. (Birmingham, AL, USA). Polyvinyl alcohol (30–70kDa, 98–99% hydrolysed; PVA), coumarin-6 and all other chemicals were purchased from Sigma Chemical Co. (St Louis, MO, USA).

Tumour cell lines

The highly metastatic murine breast cancer 4T1 cells were obtained from Dr Fred Miller, Karmanos Cancer Institute, Detroit, MI, USA. These cells were cultured in 10 cm culture plates in high-glucose Dulbecco's modified Eagles growth medium supplemented with non-essential amino acids, sodium pyruvate and 5% fetal bovine serum. The medium was changed every 3 days. The cells were passaged in a split ratio of 1 : 2 or 1 : 3.

Preparation of nanoparticles

Six different formulations (A–F) of PLGA nanoparticles, with and without the water-insoluble fluorescent marker coumarin-6, were prepared using a modified solvent evaporation method. Two different surface modifiers were used in an attempt to reduce the negative zeta potential of the particles: 0.25 mol/l calcium chloride (formulations B and E) and 0.1% chitosan (formulations C and F). Formulations D–F contained coumarin-6; formulations A–C were the control formulations and did not contain any coumarin-6.

Formulations A and D were prepared using a solvent evaporation method reported earlier.[19] In short, 500 μl Tris-EDTA (TE) buffer was emulsified in 3 ml PLGA/chloroform solution (3%), with (formulation D) or without (formulation A) 250 μg coumarin-6, using a laboratory homogeniser (PowerGen 700, Fisher Scientific, Pittsburgh, PA, USA) at 30 000 rpm for 1.5 min. The resulting primary emulsion was added drop wise to a 2% PVA solution (in 25 ml TE) and homogenised for 4 min to form a double emulsion. The second emulsification step was modified for formulations B, C, E and F: 0.25 mol/l calcium chloride was added with the PVA solution for formulations B and E; 0.1% chitosan was added with the PVA solution for formulations C and F. The mixtures were stirred magnetically (500 rpm) at room temperature for 3 h to allow complete extraction of chloroform. The final particles were collected by two-step differential centrifugation. The relatively larger particles (labelled with subscript L) were collected by centrifugation at 1000 rpm for 5 min; the relatively smaller particles (labelled with subscript S) were collected by ultracentrifugation of the supernatant at 35 000 rpm for 20 min. Fraction of the various samples were washed four times with double-distilled water to remove any residual PVA, calcium chloride and chitosan. The particles were then freeze-dried (−20°C; 6×10^{-4} mbar) for 48 h to obtain a free-flowing powder. Each formulation was prepared in triplicate.

Characterisation of nanoparticles

Particle size distribution was determined using a Mastersizer 2000 laser scattering device (Malvern Instruments Ltd., Malvern, UK). This technique measures the size of particles dispersed in a medium by the scattering pattern of a laser light shone through the medium. The size calculations assume the presence of spherical particles and the percent volume distributions assume the volumes of spheres. The samples were analysed in a water medium and the Frauenhofer method was used to calculate the size distributions. For each sample, a background run of deionised water was performed. A sample of particles (5 mg) was added to the deionised water in a small-volume sample dispersion unit. The particle size distribution was calculated after subtraction of the background. Each measurement was performed in triplicate.

Samples for scanning electron microscope (SEM) were mounted on metal stubs and the surface morphology of the particles examined using a Hitachi 3400N variable-pressure SEM (Hitachi, Gaithersburg, MD, USA). The analytical parameters included an accelerating voltage of 10 kV, a working distance of 13.5 mm and a vacuum of 40 Pa in variable pressure mode. Since the samples were analysed in variable pressure mode, the BSE2 backscatter detector was used.

The zeta potential of particles was measured using a Malvern Zeta sizer 2000 (Malvern Instruments, Malvern, UK). The experiments were performed in 10 mmol/l KCl in deionised water. All measurements were performed in triplicate.

Nanoparticle uptake study

The growth medium was aspirated from the 10 cm tissue culture dish, the cell monolayer washed with sterile phosphate-buffered saline (pH 7.4; PBS) and 1.5 ml trypsin added. The cells were then incubated at 37°C for 2–5 min to allow complete cell detachment. Fresh growth medium (10 ml) was then added and the cells flushed with a 10 ml pipette several times until all the cells were in suspension. The

suspension was transferred to a 50 ml tube and centrifuged at 1500 rpm (4°C) for 5 min to pellet the cells. The pellet was resuspended in 10 ml growth medium. A cell count was performed with a 50 μl sample of the suspension using a haemocytometer (0.1 mm deep, Bright-Line improved Neubauer, Hausser Scientific, Horsham, PA, USA).

To study the cellular uptake of nanoparticles, the 4T1 cells were seeded into a 24-well plate containing growth medium, at a density of 10 000 cells/well, and allowed to grow for 1 day.

The fluorescence intensity of coumarin-6 following cellular uptake of nanoparticles in cultured 4T1 cells was determined by fluorescence microscopy and FACS analysis. Since nanoparticle size is a determinant of their intracellular uptake, and smaller particles are known to show better uptake, we tested only the smaller nanoparticles. Three batches of blank nanoparticle preparations (formulations A_S, B_S, C_S) and three batches of fluorescent nanoparticle preparations (only D_S, E_S, and F_S) were tested. Blank nanoparticles prepared under identical conditions were used as controls. Briefly, 1×10^4 cells were seeded into two 24-well tissue culture plates in 1 ml medium. Nanoparticles were resuspended in serum-free medium at a concentration of 1 mg/ml by sonication for 30 s in a bath sonicator; 20 μl of the suspension was added to each well immediately, replacing the growth medium from the 24-well plate. The nanoparticle suspension was removed at preset sampling times (3, 24 and 48 h) and the cell monolayer was washed three times with sterile PBS to remove the unbound or undelivered nanoparticles.

Intracellular uptake of coumarin-6 into 4T1 cells was measures 24 h after treatment by fluorescence microscopy using an Olympus IX70 fluorescence microscope (Olympus, Center Valley, PA, USA) using a blue filter. Images were taken using an Olympus DP-71 digital camera.

The efficiency of intracellular delivery (internalisation) and intensity of the fluorescence was quantified using flow cytometry/FACS analysis (BD Biosciences, San Jose, CA, USA) at 405–488 nm (FITC) excitation wavelength, which is close to the excitation wavelength of coumarin-6 (390–420 nm). Briefly, 1×10^4 4T1 cells were seeded into two 24-well tissue culture plates in 1 ml medium, 1 day before the experiment. Nanoparticle suspension (20 μl) was added to each well, as described earlier, and the cells incubated for 24 h. Cells were then washed three times with 1 ml PBS and trypsinised to detach them from the wells. The cells were centrifuged at 1000 rpm for 5 min. The cell pellet was resuspended in 1 ml PBS and centrifuged at 1000 rpm for 5 min. The cell pellet was finally resuspended in 1 ml PBS and analysed by flow cytometry. Untreated cells were included as a negative control. The experiment was performed in triplicate. The efficiency of intracellular delivery of each batch of nanoparticles was determined by measuring the increase in mean fluorescence intensity.

In-vivo studies

Female Balb/c mice (8–10 weeks of age) were obtained from Charles River Laboratories (Wilmington, MA, USA). Animals were cared for in compliance with protocols approved by the Tulane University Committee on Animal Care and the 'Principles of Laboratory Animal Care' (NIH publication 85-23, revised 1985).

The biodistribution of nanoparticles in mice was studied following the protocol reported by Sasatsu and co-workers.[20] The fluorescent nanoparticles were suspended in PBS (500 μl) at a concentration of 40 mg/kg by sonicating in a bath sonicator for 30 s and were passed through a 0.8 μm syringe filter. Filtered chitosan-modified nanoparticle suspension (100 μl) was injected via the tail vein over less than 5 s using a 27-gauge needle. Mice were euthanised 24 hours later and the liver, spleen, lung, heart and kidneys collected immediately and embedded in Tissue-Tek OCT embedding compound (American Master Tek Scientific, Lodi, CA, USA) and stored in dry ice. Two sets of 12 μm thick frozen sections were cut for image analysis. One set of slides was used for fluorescence imaging and the other set was used for histological evaluation after staining with haematoxylin and eosin (H&E). For fluorescence imaging, tissue sections were washed with PBS to remove the embedding compound and a coverslip was placed with a drop of 50% glycerol.

Statistical analysis

Statistical analyses were performed using Prism software (GraphPad Software Inc., La Jolla, CA, USA). The particle size of the formulations was reported as median ± SD. The zeta potential of the formulations was compared using one-way analysis of variance (ANOVA) followed by Student–Newman–Keul's multiple comparison test. $P < 0.05$ was considered significant.

Results

Particle size distribution

A preliminary analysis showed a bimodal particle size distribution. In an effort to separate the smaller size particles from the larger ones, a two-step centrifugation process was used. The results of the particle size analysis are listed in Table 1. The median size of the particles in all formulations was between 280 nm and 7 μm. The particles that were collected by low-speed centrifugation (formulations A_L–F_L) were relatively larger, with a median size between 1.85 μm and 7 μm, whereas the particles collected by ultracentrifugation (A_S–F_S) were relatively smaller, with a median size between 280 and 872 nm. The yield of smaller size particles ranged between 50% and 66%.

In general, the particles loaded with coumarin-6 (formulations D–F) were relatively smaller than the particles that did not contain coumarin-6 (formulations A–C). The presence of calcium chloride also significantly reduced the median size from 7 μm (formulation A_L) to 4.2 μm (formulation B_L) for larger particles that did not contain coumarin-6, and from 6.2 μm (D_L) to 3.6 μm (E_L) for larger particles containing coumarin-6. The presence of chitosan also showed a similar trend for the larger particles containing coumarin-6 (i.e. $F_L < C_L$). Similar observation was also made for smaller particles of both surface modifiers, with or without coumarin-6. No significant differences were

Table 1 Particle size analysis and zeta potential of the formulations

Formulation			Median particle size (nm)	Zeta potential (mV)
A	No C6, no SM	A_L	7000 ± 400	−24.1 ± 4.6
		A_S	800 ± 200	−25.7 ± 5.0
B	No C6, SM = $CaCl_2$	B_L	4200 ± 60	−22.5 ± 4.8
		B_S	420 ± 30	−25.2 ± 4.1
C	No C6, SM = chit	C_L	2300 ± 10	−20.0 ± 4.8
		C_S	870 ± 80	−15.4 ± 4.7
D	C6, no SM	D_L	6200 ± 120	−23.7 ± 5.2
		D_S	560 ± 130	−15.3 ± 5.1
E	C6, SM = $CaCl_2$	E_L	3600 ± 40	−22.0 ± 4.7
		E_S	280 ± 10	−15.7 ± 5.0
F	C6, SM = chit	F_L	1850 ± 240	−14.5 ± 6.3
		F_S	362 ± 30	−7.0 ± 4.1

C6, coumarin-6; SM, surface modifier; $CaCl_2$, calcium chloride; chit, chitosan. Subscripts L/S denote large/small particles, respectively. Values are means ± SD (n = 3).

observed between the smaller unloaded particles with and without chitosan (C_S 870 nm, A_S 800 nm).

Surface morphology

Figure 1 shows SEM images of particles from different formulations. Larger particles prepared without any modifier (A_L and D_L) were highly porous. The porous nature of the particles was greatly reduced in the presence of calcium chloride (B_L and E_L) and completely disappeared in the presence of chitosan (C_L and F_L). The smaller particles from all the formulations (A_S–F_S) were smooth and spherical.

Zeta potential

The zeta potentials of the particles are listed in Table 1. Values were between −7 mV and −25.7 mV. Irrespective of the presence or absence of coumarin-6 or the surface modifiers calcium chloride or chitosan, the zeta potential of the larger particles did not change significantly, except formulation F_L (−14.5 mV). However, all the smaller particles containing coumarin-6 showed slightly lower zeta potentials than the corresponding larger particles. Formulation F_S showed the lowest ($P < 0.01$) zeta potential (−7 mV) among the smaller formulations.

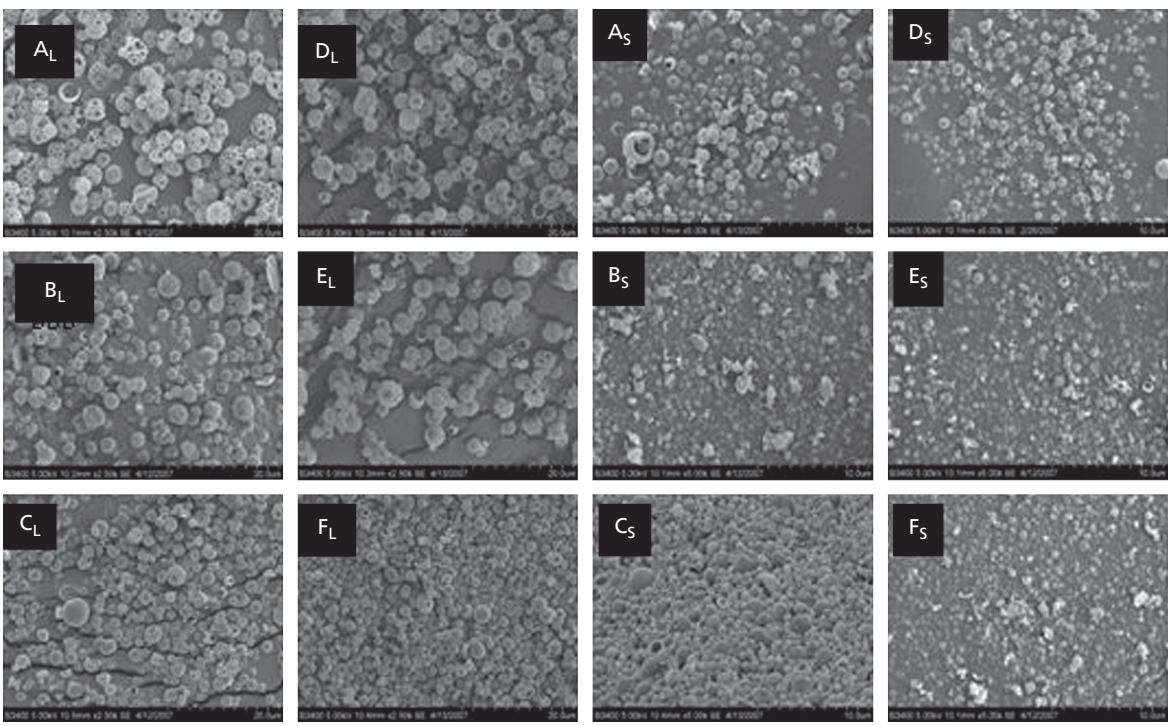

Figure 1 Scanning electron micrographs of the formulations. Large particles are denoted by subscript L and small particles by subscript S

Cellular uptake

Coumarin-6 was used as a model fluorescent compound to test the efficacy of cellular delivery of small molecules to 4T1 cells. Free coumarin-6 and unbound fluorescent nanoparticles were removed from the cell surface by washing with PBS. The efficiency of intracellular delivery of fluorescent nanoparticles was compared with that of coumarin-6 solution and unloaded blank nanoparticles. Figure 2 shows that when the cells were incubated with coumarin-6 solution, a slight fluorescence signal was observed in the cells. Similarly, a low level of fluorescence was observed when the cells were incubated with the blank nanoparticles.

When the cells were incubated with the fluorescent nanoparticles (formulations D_S, E_S and F_S) the intensity of fluorescence was high, irrespective of the relative size and surface properties of the nanoparticles (Figure 2). The fluorescence signal in these samples was captured as early as 3 h post treatment.

Closer inspection showed that coumarin-6 (encapsulated in nanoparticles as well as released) was mostly localised in cytoplasm.

Fluorescence levels were also measured quantitatively 24 h post treatment by FACS analysis. These results are summarised in Figure 3. As with fluorescence microscopy, the intensity of fluorescence in cells treated with fluorescent nanoparticles was significantly higher than in cells treated with coumarin-6 solution or unloaded (blank) nanoparticles. The formulation containing chitosan (F_S) showed the highest fluorescence intensity (192 062 a.u.) followed by the formulation modified with calcium chloride (E_S) (173 666 a.u.) and the formulation with no surface modifier (D_S) (163 280 a.u.) (Figure 3).

Biodistribution *in vivo*

Figure 4 shows the biodistribution of coumarin-6 (encapsulated in nanoparticles and already released) in selected organs of Balb/c mice 24 h after a single injection of the F_S nanoparticle formulation (chosen on the basis of cellular uptake studies). The results clearly indicated that coumarin-6 was effectively distributed to all organs examined. The intensity of the fluorescence in decreasing order was as follows: lungs (+++), heart (++), liver (+), kidney (+) and spleen (+). All of the mice survived the 24 h after injection.

Discussion

Particle size distribution

In general, the particles loaded with coumarin-6 (formulations D–F) were smaller than the particles that did not contain coumarin-6 (formulations A–C). The presence of coumarin-6 may have prevented the coalescence of emulsion droplets during the formation of the particles, maintaining a smaller particle size.

The presence of calcium chloride or chitosan significantly reduced the median size of relatively larger particles with and without coumarin-6. Both surface modifiers also reduced the size of relatively smaller particles, with or without coumarin-6.

These observations support the hypothesis that the presence of a surface modifier prevents the coalescence of emulsion droplets during particle formation and maintains a smaller particle size. No significant differences were observed between the smaller unloaded particles with and without chitosan. The increase in nanoparticle size that occurred with chitosan, in contrast to calcium chloride, may be due to the swelling property of chitosan.

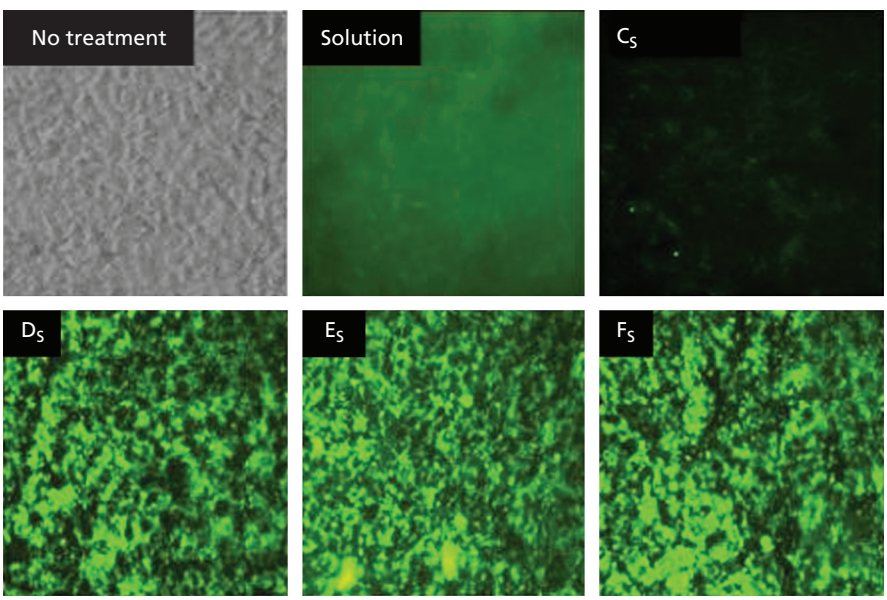

Figure 2 Fluorescence micrographs of the 4T1 breast cancer cells 24 h post treatment. Subscript S represents small-particle formulations. Each measurement was repeated three times

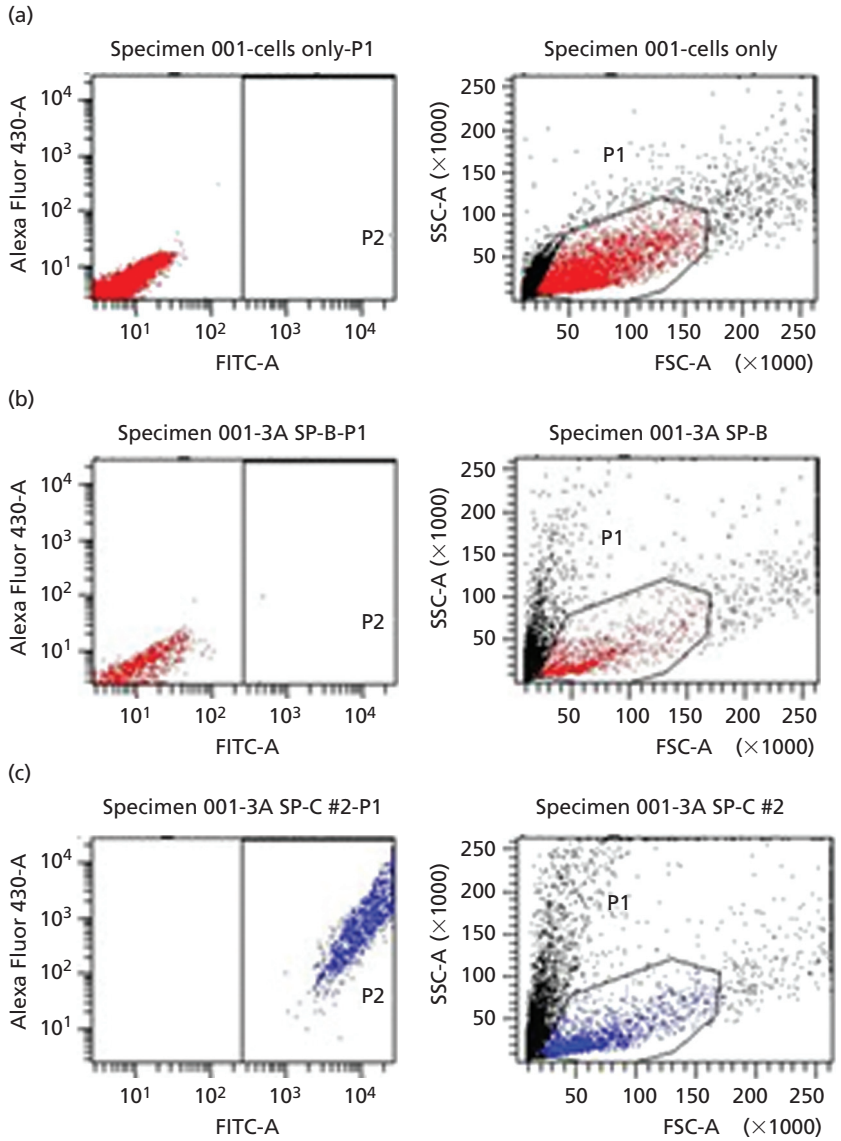

Figure 3 Flow cytometry analysis (FACS) of 4T1 breast cancer cells 24 h post treatment. (a), no treatment; (b), blank nanoparticles (formulation D_S); (c), coumain nanoparticles (formulation F_S)

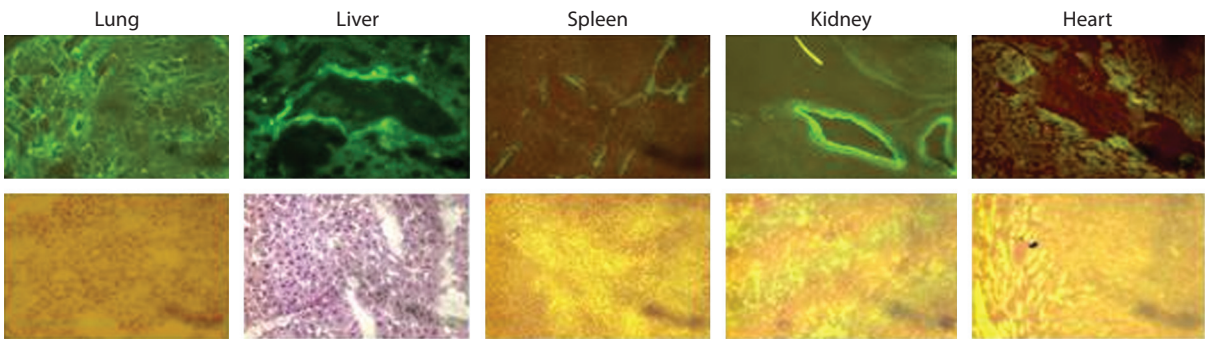

Figure 4 Biodistribution analysis of the F_S formulation (small chitosan-modified fluorescent manoparticles) in Balb/c mice following injection via a tail vein. The upper panel shows the fluorescent images of the organs 24 h post injection. The lower panel shows the histology (H&E staining) of corresponding organs to show the normal architecture

Surface morphology

Larger particles prepared without any modifier (A_L and D_L) were highly porous. The blend of Tris/EDTA buffer with the internal aqueous phase (acting as a porogen) along with the fast extraction/evaporation of chloroform (during the formation of particles) were the most likely causes of the highly porous surface of the blank as well as coumarin-6-loaded particles. The porous nature of the particles was greatly reduced in the presence of calcium chloride (B_L and E_L) and completely disappeared in the presence of chitosan (C_L and F_L). The presence of calcium chloride may have reduced the evaporation rate of the organic phase and eliminated the pores on the surface, whereas chitosan, with its superior film-forming properties, may have covered the surface of the particles with a thin film and eliminated the surface pores. The smaller particles of all the formulations (A_S–F_S) were smooth and spherical.

Zeta potential

The zeta potential of the larger particles did not change significantly irrespective of the presence or absence of coumarin-6 or the surface modifiers calcium chloride or chitosan, except formulation F_L. All the smaller particles containing coumarin-6 showed slightly lower zeta potentials than the corresponding larger particles. Formulation F_S showed the lowest zeta potential among the smaller formulations. The drastic reduction in zeta potential in these particles could be related to the small particle size: the smaller particle size will have resulted in a larger surface area and may have allowed the adsorption of a larger amount of positively charged chitosan (F_S). Between calcium chloride and chitosan, chitosan is known to have bioadhesive properties, which may have reduced the zeta potential of this formulation even further. Similer findings were also reported by other investigators.[21,22]

Cellular uptake

Coumarin-6 was used as a model fluorescent compound to test the efficacy of cellular delivery of small molecules to 4T1 cells. Coumarin-6 was also used by Khdair and co-workers[23] to study cellular uptake of nanoparticles *in vitro*. Although measurement of the fluorescent intensity of coumarin-6 is not direct proof of nanoparticle delivery within the cells, a comparison with the coumarin-6 solution does show the effect of nanoparticle-mediated delivery of coumarin-6. Cells incubated with coumarin-6 solution showed a slight fluorescence signal, as did cells incubated with blank nanoparticles. This low level of fluorescence is termed autofluorescence and is a common phenomenon, reported by Victoria and co-workers.[24] Fluorescence intensity was high when cells were incubated with the fluorescent nanoparticles (formulations D_S, E_S and F_S), irrespective of the relative size and surface properties of the nanoparticles (Figure 2). The fluorescence signal measured is due to coumarin-6 that is still encapsulated within the nanoparticles and coumarin-6 that has been released into the cells following endocytosis. However, this fluorescence was not due to coumarin-6 adhered on the surface of the cell membranes because any unbound nanoparticles and free coumarin-6 were washed off with PBS. The fluorescence signal in these samples was captured as early as 3 h post treatment, indicating that cellular uptake of these nanoparticles was rapid. The intracellular fluorescence was also monitored up to 48 h but no significant improvement in fluorescence intensity was observed after 24 h (data not shown). Closer inspection showed that coumarin-6 (encapsulated in nanoparticles as well as released) was mostly localised in the cytoplasm.

Fluorescence levels were also measured quantitatively 24 h post treatment by FACS analysis. As with fluorescence microscopy, the intensity of fluorescence in all cells treated with fluorescent nanoparticles was significantly higher than in cells treated with coumarin-6 solution or blank nanoparticles. Fluorescence intensity was highest with small chitosan particles (F_S), followed by small nanoparticles modified with calcium chloride (E_S) and those with no surface modifier (D_S). This seems to confirm earlier findings by others that the combination of smaller particle size and lower zeta potential of the F_S nanoparticle formulation improves cellular uptake. For example, Prabha and co-workers[17] reported that smaller particles showed a 27-fold higher transfection in COS-7 cell line compared with larger particles of the same composition.

Biodistribution *in vivo*

Biodistribution studies were performed with formulation F_S (chitosan-modified small fluorescence nanoparticles). Coumarin-6 was effectively distributed to all organs examined, and the intensity of the fluorescence in decreasing order was as follows: lungs (+++), heart (++), liver (+), kidney (+) and spleen (+). This study also demonstrated the feasibility of injecting the nanoparticle suspension via the tail vein in mice, and that neither the injection nor the nanoparticles caused the death of any mice within the 24 h post-treatment period.

Conclusions

The use of calcium chloride and chitosan as surface modifiers resulted in very smooth and smaller PLGA nanoparticles with reduced zeta potential. Both modifiers resulted in smaller nanoparticles that were suitable for cellular delivery. Chitosan-modified PLGA nanoparticles, size 200–400 nm with a zeta potential of −7.0 mV, showed significant uptake by 4T1 cells and were also distributed to several major cancer-relevant organs in mice following parenteral administration. The next phase of these studies will focus on the incorporation of selected anticancer drugs in the surface-modified PLGA nanoparticles for tumor-specific targeted delivery.

Declarations

Conflict of interest

The Author(s) declare(s) that they have no conflicts of interest to disclose.

Funding

This work was funded by grants from the NIH (GM08008-32 and 5P20CA118768-02), LCRC, NASA (NNC06AA18A), the Louisiana Board of Regents (RC/EEP (2007-10), LEQSF (2007-12)-ENH-PKSFI-PRS-02) and Military Infectious Disease Research Program (W81XWH-07-1-0136).

References

1. Yih TC, Al-Fandi M. Engineered nanoparticles as precise drug delivery systems. *J Cell Biochem* 2006; 97: 1184–1190.
2. Gryparis EC *et al*. Anticancer activity of cisplatin-loaded PLGA-mPEG nanoparticles on LNCaP prostate cancer cells. *Eur J Pharm Biopharm* 2007; 67: 1–8.
3. Kim ES *et al*. Human scleral diffusion of anticancer drugs from solution and nanoparticle formulation. *Pharm Res* 2009; 26: 1155–1161.
4. Suri SS *et al*. Nanotechnology-based drug delivery systems. *J Occup Med Toxicol* 2007; 2: 16.
5. Win KY, Feng SS. Effects of particle size and surface coating on cellular uptake of polymeric nanoparticles for oral delivery of anticancer drugs. *Biomaterials* 2005; 26: 2713–2722.
6. Redhead HM *et al*. Drug delivery in poly(lactide-co-glycolide) nanoparticles surface modified with poloxamer 407 and polaxamine 908: in-vitro characterization and in vivo evaluation. *J Control Release* 2001; 70: 353–363.
7. Davda J, Labhasetwar V. Characterization of nanoparticle uptake by endothelial cells. *Int J Pharm* 2002; 233: 51–59.
8. Astete CE, Sabliov CM. Synthesis and characterization of PLGA nanoparticles. *J Biomater Sci Polymer Ed* 2006; 17 : 247–289.
9. Lewis DH. Controlled release bioactive agents. In: Chasin M, Langer R (eds), *Biodegradable Polymers as Drug Delivery Systems*. New York: Marcell Dekker, 1990: 1–41.
10. Ogawa Y *et al*. Controlled release of LHRH agonist, leuprolide acetate, from microcapsules: serum drug level profiles and pharmacological effects in animals. *J Pharm Pharmacol* 1989; 41: 439–444.
11. Ramachandran R *et al*. Synthesis and characterization of PEGylated calcium phosphate nanoparticles for oral insulin delivery. *J Biomed Mat Res* 2008; $88_{[B]}$: 41–48.
12. Yang R *et al*. Lung-specific delivery of paclitaxel by chitosan-modified PLGA nanoparticles via transient formation of microaggregates. *J Pharm Sciences* 2008; 98: 970–984.
13. Youssef J *et al*. Influence of surface charge and inner composition of porous nanoparticles to cross blood–brain barrier in vitro. *Int J Pharm* 2007; 344: 103–109.
14. Zhang Y *et al*. Inhibition of peptide acylation in PLGA microspheres with water-soluble divalent cationic salts. *Pharm Res* 2009; 26: 1986–1994.
15. Desai MP *et al*. Gastrointestinal uptake of biodegradable microparticles: effect of particle size. *Pharm Res* 1996; 13: 1838–1845.
16. Demoy M *et al*. Spleen capture of nanoparticles: influences of animal species and surface characteristics. *Pharm Res* 1999; 16: 37–41.
17. Prabha S *et al*. Size-dependency of nanoparticle-mediated gene transfection: studies with fractionated nanoparticles. *Int J Pharm* 2002; 244: 105–115.
18. Sahoo SK *et al*. Residual polyvinyl alcohol associated with poly (D,L-lactide-co-glycolide) nanoparticles affects their physical properties and cellular uptake. *J Control Release* 2002; 82: 105–114.
19. Mandal TK, Tenjarla S. Preparation of biodegradable microcapsules of zidovudine using solvent evaporation: effect of the modification of aqueous phase. *Int J Pharm* 1996; 137: 187–197.
20. Sasatsu M *et al*. Preparation and biodisposition of methoxy-polyethylene glycol amine-poly(DL-lactic acid) copolymer nanoparticles loaded with pyrene-ended poly(DL-lactic acid). *Int J Pharm* 2008; 358: 271–277.
21. Cohen H *et al*. Sustained delivery and expression of DNA encapsulated in polymeric nanoparticles. *Gene Ther* 2000; 7: 1896–1905.
22. Lee D *et al*. Thiolated chitosan/DNA nanocomplexes exhibit enhanced and sustained gene delivery. *Pharm Res* 2007; 24: 157–167.
23. Khdair A *et al*. Surfactant-polymer nanoparticles enhance the effectiveness of anticancer photodynamic therapy. *Mol Pharm* 2008; 5: 795–807.
24. Victoria LM *et al*. Reducing cellular autofluorescence in flow cytometry: an in situ method. Cytometry. *Commun Clin Cytom* 1997; 30: 151–156.